

Ionic Conductivity and ^7Li NMR Study of Solid Polymer Electrolytes Based on Polyetherurethane Copolymer Networks

Dong-Won KIM, Jung-Ki PARK[†], Hee-Woo RHEE,*
and Hong-Doo KIM**

*Department of Chemical Engineering, Korea Advanced Institute of Science and Technology,
373-1, Kusung-Dong, Yuseong-Gu, Daejeon 305-701, Korea*

**Department of Chemical Engineering, Sogang University,
1-1 Shinsoo-Dong, Mapo-Gu, Seoul 121-742, Korea*

***Department of Chemistry, Kyunghee University, Suwon, Korea*

(Received November 22, 1993)

ABSTRACT: Crosslinked polyetherurethane (PEU) copolymer networks consisting of the low molecular weight poly(ethylene oxide) (PEO) and poly(propylene oxide) (PPO) segments with an aliphatic diisocyanate were synthesized and complexed with a LiClO_4 salt to form solid polymer electrolytes. The ionic conductivities of these samples were measured as a function of PEO composition at various temperatures. And a solid ^7Li NMR relaxation technique was used as a means of understanding the local environments and dynamics of the lithium ions in the polymer electrolytes. The difference in spin-spin relaxation times (T_2) between two spectral components enabled to their separation, and thus we could monitor the mobile Li^+ ion concentration and its motion as a function of PEO composition and temperature.

KEY WORDS Copolymer Network / Ionic Conductivity / ^7Li NMR Relaxation / Polyetherurethane / Poly(ethylene oxide) / Polymer Electrolyte / Poly(propylene oxide) /

Polymer electrolytes have been received a considerable attention as solid electrolyte materials in the advanced applications such as high energy-density batteries, electrochromic devices, chemical sensors and photoelectrochemical cells.^{1,2} The great deal of studies to date have been carried out on polymer electrolytes based on poly(ethylene oxide) (PEO) containing the lithium salts. However, their high crystallinity decreases the ionic conductivity to a level too low to satisfy the requirement of room temperature applications, since conductivity in semi-crystalline polymer electrolytes is mainly achieved through the amorphous phase in complexes.^{3,4} Various attempts have been made to prepare the solid polymer electrolytes with the improved ionic

conductivities and dimensional stability at ambient temperature.⁵⁻²⁰ Among them, the synthesis of crosslinked polyether-urethane was found to provide a means to inhibit the crystallization and to improve the mechanical strength. The most prominently reported networks were those arising from the reaction of polyfunctional isocyanates with homopolyols poly(ethylene glycol) (PEG) only^{12-15,19,20} or poly(propylene glycol) (PPG) only^{12,14,16-18}. It is conceivable that the controlled compositional changes in the polyether segments composed of both PEO and poly(propylene oxide) (PPO) affect the carrier generation and migration in polymer electrolytes prepared with them.

In this study, we prepared the polyether-

[†] To whom correspondence should be addressed.

urethane copolymer networks composed of both a crystalline PEO and an amorphous PPO. The presence of ethylene oxide (EO) units is expected to make these networks better solvent for polymer electrolyte materials, while the propylene oxide (PO) units can inhibit the crystallization of polyetherurethane (PEU) networks. We changed the composition of polyether segments in order that ionic conductivities of the polymer electrolytes could be optimized.

The application of NMR techniques in polymer electrolyte studies has been a potentially powerful tool for exploring both the structural and dynamic nature of polymer electrolytes.^{13,21–28} Especially, the correlation of the conductivity with ionic motion in microscopic level could be envisioned through NMR relaxation studies. Thus, we carried out the ⁷Li NMR relaxation experiments for investigating the temperature and PEO composition dependence of the spin–spin relaxation times and fractions for the mobile Li⁺ ions, and correlated these measurements with conductivity results.

EXPERIMENTAL

Materials

Triol type PPO (MW: 3000) was obtained from Korea Polyol Co. and the volatile compounds in the sample were removed under reduced pressure at 80°C for 6 h before use. Commercial sample of diol type PEO (MW: 2000) was supplied by Aldrich Chemicals Co. and used without any further purification. Their chemical structures and DP were checked by ¹H NMR spectroscopy. Anhydrous LiClO₄ supplied by Aldrich Chemicals Co. was dried at 120°C in a vacuum oven overnight.

PEU networks were prepared by the crosslinking reaction of PPO triol and PEO diol with hexamethylene diisocyanate (HDI) in the presence of small amounts of dibutyltin dilaurate as a catalyst. With respect to the functional groups, stoichiometric amounts of

PEO, PPO were mixed sufficiently with excess amount of HDI for driving the faster chain extension rate in dichloromethane, and the reacting solution was poured into the glass substrate. The crosslinking reaction occurred at 80°C under dry nitrogen atmosphere for 48 h. The reaction rate seemed to be moderate, since the used diisocyanate in this reaction was not aromatic but aliphatic. However, the network structures based on aliphatic diisocyanate are expected to have a higher flexibility than the polyether networks based on aromatic diisocyanate such as toluene diisocyanate (TDI), since the crosslinking points having aromatic rings tend to make resulting polymer rather rigid, and consequently the segment motion of the polymer chain is somewhat inhibited. The crosslinked PEU elastomers are washed twice with acetone to remove completely the residual soluble low molecular fractions, and then dried in a vacuum oven at 80°C for 24 h. In this study, polyetherurethanes in the weight ratio of polyols in the feed (PEO:PPO), 0:10, 2:8, 4:6, 6:4, 8:2, 10:0 were prepared. The PEU network samples are designated as PEU_x, where *x* means the relative PEO weight ratio with respect to the total polyethers (*i.e.*, PEO and PPO). It should be noted that PEU 100 has the linear structure instead of three dimensional form, since only linear PEO diol and HDI are used in the absence of PPO triol.

Preparation of Polymer Electrolytes

The pre-weighted PEU networks are swollen in solutions of LiClO₄ in acetone allowing the salt to diffuse into the network films. They are dried at 60°C under vacuum and weighed again. In order to ensure a uniform dissolution of LiClO₄ through the polymer film, immersion was continued until the weight change of the film before and after immersion reached a constant level. The weight difference then gives the concentration of salt dissolved in the polymer electrolytes. In this study, the concentration of salt in all of the polymer

electrolytes was fixed to be constant ($\text{Li}^+/\text{O} \cong 0.075$) in order to neglect the effect of salt concentration.

Conductivity Measurement

Polymer electrolyte films were sandwiched between two stainless steel electrodes (12 mm in diameter). The ionic conductivity of the polymer electrolyte film was measured by complex impedance analysis using a Solatron 1255 frequency response analyzer coupled to an IBM PS/2 computer over a frequency range of 0.1 Hz–10 MHz. The real and imaginary parts of the complex impedance were plotted, and the ionic conductivity (σ) could be obtained from the bulk resistance (R_b) found in complex impedance diagram.

^7Li NMR

The solid state ^7Li NMR experiments were performed on a Bruker-MSL-200 NMR spectrometer with a magnetic field of 4.7 T corresponding to a ^7Li resonance frequency of 77.7 MHz. The polymer electrolyte film was transferred into a NMR tube, subsequently sealed to prevent access of humidity to the sample. The spin–spin relaxation time (T_2) was determined using the spin–echo technique by applying $90^\circ\text{--}\tau\text{--}90^\circ$ pulse sequences and observing an echo at time 2τ . The temperature of the sample was controlled to within $\pm 1.0^\circ\text{C}$ with a Bruker temperature regulating system in the temperature region $298 \sim 348$ K.

Thermal Analysis

The differential scanning calorimetry (DSC) studies were carried out to determine the glass transition or melting temperature of the sample using a Du Pont 9900 instrument. Samples were loaded in hermetically-sealed aluminum pans and measurements were taken over a temperature range of -100 to 100°C at a heating rate of $20^\circ\text{C min}^{-1}$. The recorded T_g was taken as the inflection point and T_m was given as the peak temperature of the melting endotherm.

RESULTS AND DISCUSSION

DSC Analysis

The representative DSC thermograms of PEG, PPG, and PEU 40 are shown in Figure 1, and the DSC results are summarized in Table I. The degree of crystallinity for the PEO diol was about 88%, and T_g could not be detected. For the PPO triol and the pure PPO network (PEU 0), the melting could not be observed, indicating that they were completely amorphous. With the incorporation of PEO in PEU network, melting peak appeared, and both the values of T_m and ΔH_m increased with PEO composition. However the crystallinity of PEO in PEU copolymer networks was significantly reduced as compared with PEO homopolymer, which is probably due to the crosslinking with an amorphous PPO. The melting temperatures of the PEU copolymer networks were near the

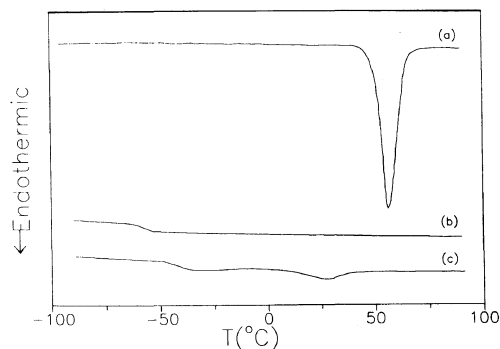


Figure 1. DSC thermograms of PEG, PPG, and PEU 40: (a) PEG; (b) PPG; (c) PEU 40.

Table I. The DSC results of PEO diol, PPO triol, and PEU networks

| Sample | T_g | T_m | ΔH_m | Crystallinity/% |
|----------|-------|-------|--------------|-----------------|
| PEO 2000 | | 57 | 179.3 | 88 |
| PPO 3000 | -58 | | | |
| PEU 0 | -39 | | | |
| PEU 20 | -39 | 21 | 2.0 | 1 |
| PEU 40 | -43 | 26 | 8.6 | 4 |
| PEU 60 | -45 | 26 | 20.2 | 10 |
| PEU 80 | -46 | 24 | 36.4 | 18 |
| PEU 100 | -50 | 30 | 45.7 | 23 |

Table II. The DSC results of polymer electrolytes based on PEU networks

| Polymer electrolytes | T_g | ΔT_g^a | T_m | ΔH_m | LiClO ₄ wt% | Li ⁺ /O |
|----------------------------|-------|----------------|-------|----------------------|------------------------|--------------------|
| PEU 0/LiClO ₄ | -25 | 14 | | | 11.1 | 0.076 |
| PEU 20/LiClO ₄ | -24 | 15 | | | 13.1 | 0.086 |
| PEU 40/LiClO ₄ | -23 | 20 | | | 12.2 | 0.075 |
| PEU 60/LiClO ₄ | -20 | 25 | | | 12.8 | 0.074 |
| PEU 80/LiClO ₄ | -13 | 33 | | | 13.5 | 0.075 |
| PEU 100/LiClO ₄ | -11 | 39 | 28 | 8.2 (4) ^b | 13.8 | 0.073 |

^a ΔT_g represents the difference of T_g between the pure PEU network and the PEU/LiClO₄ complex.

^b The value in the parenthesis means the crystallinity estimated with heat of fusion (ΔH_m).

room temperature (21–30°C), and thus these polymers seemed to exhibit the amorphous structure at the room temperature. It was also found that the T_g values of PEUs decreased with PEO content. This result may be due to the fact that the crosslinking density decreases with the content of linear flexible PEO chain. With the DSC results, the phase separation between the two phases (PEO and PPO) could not be observed.

The DSC results of polymer electrolytes prepared with same LiClO₄ concentration are given in Table II. The PEU 100/LiClO₄ complex shows a melt transition in addition to the glass transition. However, the other PEU/LiClO₄ complexes exhibit only the glass transition in the DSC thermograms, which indicates that these complexes become completely amorphous by incorporating of LiClO₄. The data in this table also exhibit a larger value of ΔT_g with increasing the PEO content, which probably results from the stronger solvating property of the EO unit in comparison to the PO unit in the network. Ionic dissociation is relatively restrained in PPO as compared to PEO phase, because the dielectric constant of PPO is lower than that of PEO, and the bulky methyl groups in PPO hamper the interaction between the lithium cations and the oxygen atoms on PPO. The strong ion–dipole interaction in PEO-rich network, thus, provokes a more significant reduction (ΔT_g) in the polyether segmental mobility as compared to PPO-rich network at same salt concentration.

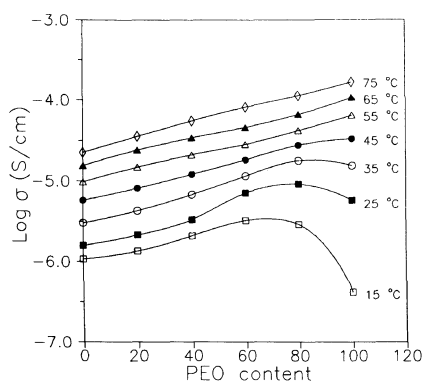


Figure 2. Ionic conductivities of PEU/LiClO₄ complexes as a function of PEO composition in copolymer networks at various temperatures.

Ionic Conductivity

Figure 2 shows the conductivity variations as a function of PEO composition in the temperature range of 15–75°C. The optimum PEO composition at which the conductivity passes through a maximum was observed below 35°C. This behavior may be related to the number of charge carriers, the ionic mobility related with ion–polymer interaction and the crystallinity of polymer electrolyte. There is a build up of charge carriers as the PEO content is increased, since the abundance of EO units makes these materials better solvents for dissolving LiClO₄ as explained above. However, the slight decline of conductivity may be due to the absence of PO units to function as irregularities which inhibit crystallization of the polymer electrolytes, since

ionic transport is impeded in the crystalline region. Moreover, the strong ion–polymer interaction in PEO-rich PEU networks can reduce the ionic mobility. Thus, the appearance of the maximum conductivity can be attributed the addition of two opposing effects. As can be seen in this figure, polymer electrolyte containing 80% PEO has the highest conductivity of about $7.2 \times 10^{-6} \text{ S cm}^{-1}$ at room temperature. This result suggests that the proper change of network composition can bring about an increase of the ionic conductivity at ambient temperature. However, at higher temperature, the increase of free volume due to the destruction of crystallinity as well as the weaker ion–polymer interaction could lead to an easier ionic diffusion. The continuous increase of conductivity with PEO content, thus, may be related to the increase in carrier concentration as well as carrier migration. From the temperature dependence of ionic conductivity of each sample, it is observed that activation energy is increasing as a function of PEO composition in solid polymer electrolytes.

^7Li NMR

The ^7Li NMR experiments were undertaken to supplement the information obtained from the measurement of ionic conductivity. The ^7Li NMR spectrum of the solid polymer electrolyte was a superposition of a narrow component and a considerably broader component. The reasonable source of narrow component with longer T_2 is a highly mobile lithium ion (which is contribute to the ionic conduction), while the broad component with shorter T_2 is attributed to tightly bound lithium species (ion-pairs that have aggregated into clusters) just as we have already reported.^{9,28} In fact, ion pairing and ion aggregation are expected to slightly immobilize the Li^+ ions, which result in broadening the line shapes. The T_2 values and relative intensities of these samples were estimated from the plot of the echo intensity vs. decay time (2τ) as shown in Figure 3. Decomposition of the multiple decays into two

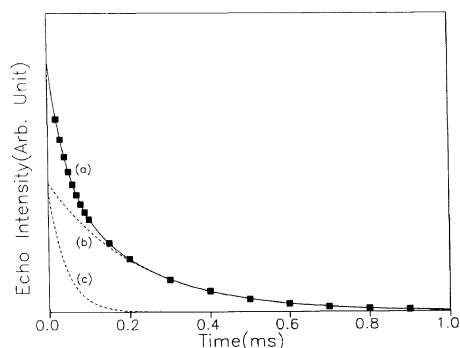


Figure 3. ^7Li echo intensity vs. decay time for PEU 60/ LiClO_4 at 25°C : (a) overall intensity (The symbols represent the solid echo data and the solid line is sum of two components resolved); (b) slow component (long T_2) resolved from overall intensity; (c) fast component (short T_2) resolved from overall intensity.

Table III. The fraction of free lithium ions and the spin–spin relaxation times in PEU/ LiClO_4 complexes at 25°C

| Polymer electrolyte | x_F | T_{21}^a | T_{22}^b |
|---------------------|-------|------------|------------|
| | | ms | ms |
| PEU 0 | 0.06 | 0.10 | 0.01 |
| PEU 20 | 0.18 | 0.13 | 0.02 |
| PEU 40 | 0.33 | 0.14 | 0.02 |
| PEU 60 | 0.52 | 0.22 | 0.04 |
| PEU 80 | 0.59 | 0.19 | 0.04 |
| PEU 100 | 0.66 | 0.12 | 0.03 |

^a Spin–spin relaxation time of the free mobile lithium nucleus in polymer electrolyte.

^b Spin–spin relaxation time of the tightly bound lithium nucleus in polymer electrolyte.

components followed the established procedure.⁹ The T_2 values and relative intensities (x_F) of free mobile lithium ions estimated from the two resolvable components at 25°C are summarized in Table III. From the data in this table, it is found that x_F ranges from 0.06 to 0.66 as a function of PEO composition. It therefore seems unlikely that there would be a complete dissociation of added salt in solid polymer electrolytes. In fact, since the dielectric constants of these samples are rather low ($\epsilon = 8.1$ – 10.6 , from impedance analyses at

room temperature), the dissociation is expected to be incomplete. And it is shown that x_F increases with PEO content in PEUs. The increase in the number of charge carriers with PEO composition is probably attributed to the better solvating property of the EO unit than that of the PO unit. This result was previously confirmed with the change of T_g by the DSC analysis of polymer electrolytes. It is also found that the T_{21} value proportional to the mobility of free mobile lithium ion increases as the PEO composition increases up to 60, and it decreases beyond the maximum with further increasing PEO content. This phenomenon is closely related with the ion-polymer interaction in polymer electrolytes. The number of crosslinking points decreases and the amount of linear flexible EO units increases with PEO content, and thus the ionic mobility increases up to 60% PEO composition. While the decline in T_{21} beyond the maximum is probably associated with the reduction of mobilities of free mobile cations due to the strong ion-polymer interaction promoting the salt solvation. Thus, it is concluded that the drop in ambient temperature conductivity at higher PEO content (Figure 2) is related to the decreasing of ionic mobility rather than the number of charge carriers. These results suggest that the balance should be required for optimum conductivity in polymer electrolyte in which the ion-polymer interactions must be sufficiently strong to generate the charge carriers (free mobile ions), but excessively strong association may suppress the ionic motion at ambient temperature in this system.

With the solid echo data as a function of temperature, the fraction of free lithium ions (x_F) and their spin-spin relaxation times (T_{21}) could be also estimated at various temperatures. Only the fraction of free Li^+ ions which have long T_2 values (x_F) is responsible for the ionic conduction, the temperature dependence of x_F may be explained by a dissociation equilibrium. The relative intensities of the free

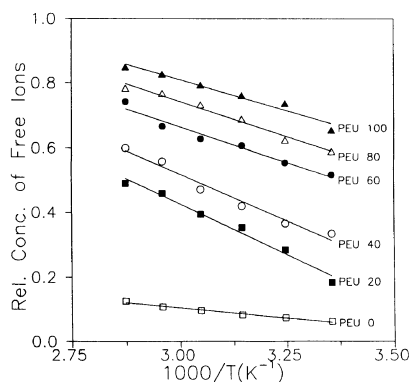


Figure 4. The relative concentration of free mobile lithium ion vs. reciprocal temperature in polymer electrolytes.

mobile lithium nuclei for all the polymer electrolytes considered in our study as a function of reciprocal temperature are plotted in Figure 4. From Figure 4, it is clearly found that the number of charge carriers is increased with increasing PEO composition over all the temperature range studied. These NMR results indicate that the number of free mobile ions which contribute to the ionic conductivity is always more abundant in PEO-rich PEU complex, which may be related to the better solvating power of PEO than that of PPO as explained above. It is also found that there is an increase in mobile lithium ions with increasing temperature. If these phenomena are interpreted as a temperature dependent ion dissociation process, it is apparent that the total carrier concentration changes by only a small amount in the temperature range of 25–75°C. Especially, it is noted that the fraction of mobile lithium ions of PEU 0/ LiClO_4 complex can be compared with that previously reported for crosslinked PPO/ LiClO_4 complex by Watanabe *et al.*,¹⁸ although the chemical structures between two systems are different in terms of diisocyanate linkages. They reported that the degree of dissociation of LiClO_4 calculated from the ionic mobility measurement in PPO network with TDI linkage was 1.5–6.0% at the temperature ranges of 43–98°C, while its

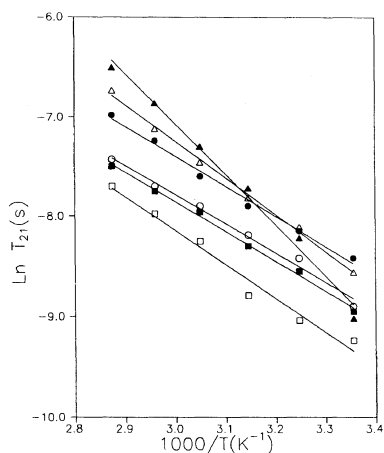


Figure 5. Arrhenius plot of the ${}^7\text{Li}$ spin-spin relaxation times of free mobile lithium ions in polymer electrolytes: \square , PEU 0; \blacksquare , PEU 20; \circ , PEU 40; \bullet , PEU 60; \triangle , PEU 80; \blacktriangle , PEU 100.

Table IV. The activation energies estimated from the ionic conductivities and ${}^7\text{Li}$ NMR results in the temperature range of 25–75°C

| Polymer electrolyte | E_a (eV) calculated from ionic conductivity | E_a (eV) calculated from ${}^7\text{Li}$ NMR |
|---------------------------|---|--|
| PEU 0/ LiClO_4 | 0.36 | 0.28 |
| PEU 20/ LiClO_4 | 0.39 | 0.26 |
| PEU 40/ LiClO_4 | 0.38 | 0.25 |
| PEU 60/ LiClO_4 | 0.34 | 0.26 |
| PEU 80/ LiClO_4 | 0.40 | 0.32 |
| PEU 100/ LiClO_4 | 0.59 | 0.44 |

value was shown to be 6.2–12.6% from our ${}^7\text{Li}$ NMR relaxation measurement at the temperature ranges of 25–75°C.

The T_{21} values associated with the mobilities of free lithium ions as a function of temperature are also shown in Figure 5. From the plot of $\ln(T_{21})$ vs. $1/T$, the activation energies for ionic migration are calculated. In an attempt to compare these results with the ones obtained from conductivity measurements, the activation energies are also approximately calculated from the $\ln \sigma$ vs. $1/T$ by using the conductivity data in Figure 2, the results are summarized in Table IV. It is noteworthy that NMR ac-

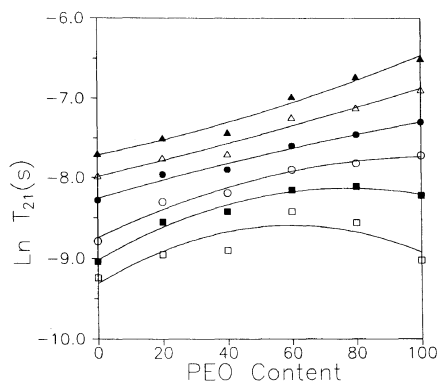


Figure 6. The ${}^7\text{Li}$ spin-spin relaxation times of free mobile lithium ions as a function of PEO composition at various temperatures: \square , 25; \blacksquare , 35; \circ , 45; \bullet , 55; \triangle , 65; \blacktriangle , 75°C.

tivation energies are always lower than conductivity activation energies, probably due to the sensitivity of ${}^7\text{Li}$ NMR to only localized motions. That is to say, the activation energies obtained from ${}^7\text{Li}$ NMR results do not include the ion–ion and ion–polymer interactions as well as the temperature dependence of the number of carrier ions, which must be considered in conductivity measurements. It is also important to note that the T_{21} value (Figure 5) increased about an averaged factor of 6.4 from 25 to 75°C, while the concentration of free ions (Figure 4) increased by only a factor of 1.8 within the same temperature range. These results suggest that the ionic transport plays a much greater role than carrier generation according to the variation of temperature in ionic conductivity mechanism. A similar conclusions have been also drawn by Wintersgill *et al.*²⁹ (from the ${}^{23}\text{Na}$ NMR measurement in crosslinked DMS–EO copolymer/ NaCF_3COO complex) and Watanabe *et al.*¹⁸ (from the mobility measurement in crosslinked PPO/ LiClO_4 complex).

The influence of PEO composition on ionic mobility (T_2) at a given temperature is well represented in Figure 6. It is found that there is a PEO composition at which the T_{21} value passes through a maximum, just as the change

in conductivity with PEO composition shows a maximum at lower temperature. This maximum is shown to be displaced to higher PEO composition as the temperature increases. At higher temperature, the increase of free volume due to the destruction of crystallinity and weaker salt-polymer interaction according to increase of temperature leads to an easier ionic migration in spite of abundance in charge carriers in PEO-rich PEU complex which has lower degree of crosslinking density. From the results discussed with the above ^7Li NMR and conductivity data, we can suggest with confidence that the larger concentration of free mobile ions and the higher ionic mobility in PEO-rich PEU/ LiClO_4 complex than in PPO-rich PEU/ LiClO_4 complex gives rise to a larger conductivity at higher temperature, while the restriction of ionic mobility due to the strong ion-polymer interaction causes the reduction of ionic conductivity in spite of abundance in the number of charge carriers at lower temperature.

CONCLUSION

Polyetherurethane networks consisting of a crystalline PEO and an amorphous PPO were synthesized and complexed with a LiClO_4 salt. Variation of the PEO/PPO ratios in the PEU copolymer networks enabled to optimization of ionic conductivity at lower temperature (15–35°C), while the continuous increase in conductivity was observed with increasing of PEO content at higher temperature (45–75°C) range. For all the systems studied in our study, the ionic conductivity values were higher than 10^{-6} Scm^{-1} at 25°C. The ^7Li NMR relaxation results in PEU networks showed that the lithium ions existed in at least two environments, indicating that the presence of a mobile lithium species as well as a less mobile component confined in the polymer network. We could monitor the relative ionic mobility and the fraction of free mobile ions contributing to the ionic conductivity as a function of

PEO composition and temperature.

Acknowledgment. This work has been carried out with the Korean Ministry of Education Research Fund for Advanced Materials in 1992.

REFERENCES

1. J. R. MacCallum and C. A. Vincent, Ed., "Polymer Electrolyte Reviews," Vol. 1 and 2, Elsevier Applied Science, London, 1987 and 1989.
2. J. S. Tonge and D. F. Shriver in "Polymers for Electronic Applications," J. H. Lai, Ed., CRC Press, Inc., Boca Raton, Florida, 1989.
3. C. C. Lee and P. V. Wright, *Polymer*, **23**, 681 (1982).
4. J. E. Weston and B. C. H. Steele, *Solid State Ionics*, **7**, 75 (1982).
5. P. M. Blonsky, D. F. Shriver, P. Austin, and H. R. Allcock, *J. Am. Chem. Soc.*, **106**, 6854 (1984).
6. D. J. Bannister, G. R. Davies, I. M. Ward, and J. E. McIntyre, *Polymer*, **25**, 1600 (1984).
7. F. M. Gray, J. R. MacCallum, C.A. Vincent, and J. R. M. Giles, *Macromolecules*, **21**, 392 (1988).
8. M. Seki, K. Sato, and R. Yosomiya, *Makromol. Chem.*, **193**, 2971 (1992).
9. D. W. Kim, J. K. Park, M. S. Gong, and H. Y. Song, *Polymer Eng. Sci.*, in press (1994).
10. S. Pantaloni, S. Passerini, F. Croce, and B. Scrosati, *Electrochimica Acta.*, **34**, 635 (1989).
11. D. Fish, I. M. Khan, and J. Smid, *Makromol. Chem. Rapid Commun.*, **7**, 115 (1986).
12. A. Killis, J. F. Lenest, A. Gandini, and H. Cheradame, *J. Polym. Sci., Polym. Phys. Ed.*, **19**, 1073 (1981).
13. A. Killis, J. F. Lenest, A. Gandini, H. Cheradame, and J. P. C. Addad, *Polym. Bull.*, **6**, 351 (1982).
14. M. Leveque, J. F. Lenest, A. Gandini, and H. Cheradame, *Makromol. Chem. Rapid Commun.*, **4**, 497 (1983).
15. A. Killis, J. F. Lenest, A. Gandini, and H. Cheradame, *Macromolecules*, **17**, 63 (1984).
16. M. Watanabe, S. Oohashi, K. Sauni, N. Ogata, T. Kobayashi, and Z. Ohtaki, *Macromolecules*, **18**, 1945 (1985).
17. M. Watanabe, K. Sauni, N. Ogata, F. Inoue, T. Kobayashi, and Z. Ohtaki, *Polym. J.*, **4**, 549 (1985).
18. M. Watanabe, K. Sauni, N. Ogata, T. Kobayashi, and Z. Ohtaki, *J. Appl. Phys.*, **57**, 123 (1985).
19. M. Watanabe, S. Nagano, K. Sauni, and N. Ogata, *Polym. J.*, **18**, 809 (1986).
20. Y. Kato, M. Watanabe, K. Sauni, and N. Ogata, *Solid State Ionics*, **40/41**, 632 (1990).
21. S. G. Greenbaum, *Solid State Ionics*, **15**, 259 (1985).
22. W. Gorecki, R. Andreani, C. Berthier, M. Armand,

- M. Mali, J. Roos, and D. Brinkmann, *Solid State Ionics*, **18/19**, 295 (1986).
23. S. G. Greenbaum, Y. S. Pak, M. C. Wintersgill, J. J. Fontanella, J. W. Schultz, and C. G. Andeen, *J. Electrochem. Soc.*, **135**, 1 (1988).
24. Y. S. Pak, K. J. Adamic, S. G. Greenbaum, M. C. Wintersgill, J. J. Fontanella, and C. S. Coughlin, *Solid State Ionics*, **45**, 277 (1991).
25. J. F. O'Gara, G. Nazri, and D. M. MacArthur, *Solid State Ionics*, **47**, 87 (1991).
26. S. H. Chung, K. R. Jeffrey, and J. R. Stevens, *J. Chem. Phys.*, **94**, 1803 (1991).
27. W. Gang, J. Roos, D. Brinkmann, F. Capuano, F. Croce, and B. Scorasati, *Solid State Ionics*, **53/56**, 1102 (1992).
28. D. W. Kim, B. K. Ryoo, J. K. Park, K. S. Maeng, and T. S. Hwang, *Polym. J.*, **24**, 509 (1992).
29. M. C. Wintersgill, J. J. Fontanella, M. K. Smith, S. G. Greenbaum, K. J. Adamic, and C. G. Andeen, *Polymer*, **28**, 633 (1987).